

Photochemistry of ZnTPP induced by cadmium sulfide nanoparticles in 2-propanol

Bhamro, John Chrysochoos

Department of Chemistry, The University of Toledo, Toledo, OH 43606, USA

Accepted 4 July 1997

Abstract

Addition of ZnTPP to non-stoichiometric CdS nanoparticles in 2-propanol leads to adsorption of ZnTPP molecules onto the surface of the nanoparticles. A limiting adsorption of about 13% ZnTPP molecules onto the surface of 2×10^{-4} M CdS nanoparticles was determined by ultrafiltration (100 Å membrane filters). It corresponds to $6.15 \times 10^{-4} \times m$ ZnTPP molecules adsorbed onto the surface of an average-size CdS nanoparticle; m is the number of CdS units in such a nanoparticle. Both the quenching of the recombination luminescence of CdS (e_{ic}^- / h_{ir}^+) by ZnTPP and the photoreactivity of ZnTPP in the presence of CdS nanoparticles are linked to the extent of adsorption of ZnTPP onto CdS. The adsorption of ZnTPP onto the surface of CdS nanoparticles is described by Langmuir-type plots. UV irradiation of ZnTPP in the presence of CdS nanoparticles leads to the formation of intermediate photoproducts, characterized with absorption bands in the red region of the spectrum, which subsequently convert to more stable photoproducts. The former photoproducts are attributed to reactions of O_2^- with ZnTPP whereas the latter may be linked to the reduction of ZnTPP, substitution at the exodouble bonds of ZnTPP and to open macrocyclic structures. © 1997 Elsevier Science S.A.

Keywords: Nanoparticles; Cadmium sulfide; Zinc tetraphenylporphyrin

1. Introduction

Semiconductor nanoparticles are characterized by size-dependent optical and photoredox properties [1,2]. Because of the size dependence of their photoredox properties, semiconductor nanoparticles have been used extensively to probe light-induced interfacial electron transfer and heterogeneous photocatalysis, in general [3–7]. The primary step in heterogeneous photocatalysis is tacitly assumed to involve interfacial electron transfer. Electron transfer from the conduction band of semiconductor particles to electron acceptors can be monitored by recombination luminescence quenching of the semiconductor nanoparticles brought about by the reducible electron acceptors (quenchers) [8–12], by EPR spectroscopy [13], by the formation of primary (transient) photoproducts [14,15], and by other techniques.

Although the efficiency of the recombination luminescence quenching of CdS nanoparticles by Ln^{3+} ions was found to depend upon the redox potential of the ions, $E^\circ(Ln^{3+}/Ln^{2+})$, the relative quenching efficiency of metalloporphyrins (MTPP, M = Mg, Zn, Cd, Ni, Cu, Co) does not follow the trend of the redox potentials of MTPP [12]. The latter observation implies that MTPP molecules are adsorbed to a different extent onto the surface of CdS nanoparticles,

depending upon the metal ion inserted into the cavity of the porphyrin, and on its coordination. Interfacial electron transfer from CdS(e^-/h^+) nanoparticles to MTPP molecules, adsorbed onto the surface of the nanoparticles, may take place provided it is thermodynamically allowed:

$$\Delta G_{cl,ir}^\circ = eE^\circ(e_{cB}^-) - eE^\circ(MTPP/MTPP^-) - e^2/\epsilon R < 0 \quad (1)$$

The redox potential of the electron in the conduction band of CdS nanoparticles, $E^\circ(e_{cB}^-)$, is more negative than that of the electron in the conduction band of bulk CdS, by $h^2/2m_c e R^2$ V. This is attributed to the 'space confinement' of e_{cB}^- in the nanoparticle which leads to an increase in the bandgap energy of the semiconductor nanoparticle as its size decreases [16].

$$E_{e^-}(\text{particle}) = E_g(\text{Bulk}) + (\hbar^2 \pi^2 / 2R^2) \times (1/m_c^* + 1/m_h^*) - 1.8e^2/\epsilon R + \text{polarization terms} \quad (2)$$

Consequently, both the quenching of the recombination luminescence of CdS nanoparticles by metalloporphyrins and the resulting photoreactivity of MTPP need to be considered in terms of interactions of MTPP with the surface of the nanoparticles. Such interactions lead to surface modification of CdS nanoparticles which may facilitate electron transfer or

may alter the properties of the nanoparticles by forming new energy levels in the bandgap of the semiconductor [13]. This paper deals with the adsorption characteristics of ZnTPP onto the surface of CdS nanoparticles and the photoreactivity of ZnTPP induced by CdS.

2. Experimental

Cadmium sulfide nanoparticles were prepared in 2-propanol at -78°C without added stabilizers using well established literature methods of 'arrested precipitation' [17]. The preparation was carried out by a rapid mixing of a solution of 1.2×10^{-3} M $\text{Cd}(\text{ClO}_4)_2 \cdot 6\text{H}_2\text{O}$ in 2-propanol with a freshly prepared solution of Na_2S in a mixture of 2-propanol-methanol (6:1 V/V) in the presence of an excess of NaOH . Both solutions were precooled and deaerated before mixing. The semiconductor nanoparticles prepared in this way had a $[\text{Cd}^{2+}]/[\text{S}^{2-}]$ ratio equal to 3 (non-stoichiometric CdS nanoparticles). Different preparations were characterized as 4:8:4, namely 4×10^{-4} M CdS, 8×10^{-4} M Cd^{2+} excess and 4×10^{-1} M NaOH , or 2:4:2.

The optical bandgap of CdS nanoparticles (E_g) was calculated from the absorption coefficient, $\alpha(h\nu)$, of the edge-to-edge absorption band of the nanoparticle associated to direct transitions in CdS, namely transitions from the top of the valence band ($k=0$) to the bottom of the conduction band ($k=0$) [18,19].

$$\alpha(h\nu) = \left\{ e^2 (2m_h^* m_e^* / (m_h^* + m_e^*))^{1/2} / nch^2 m_e^* \right\} (h\nu - E_g)^{1/2} \quad (3)$$

where m_h^* and m_e^* are the effective masses of the hole and the electron, respectively; E_g values were found to range from 2.9 to 3.1 eV from the straight lines of the plots $\{\alpha(h\nu)\}^2$ vs. $h\nu$ (eV) as $\alpha(h\nu) \rightarrow 0$.

Ultraviolet and visible absorption spectra were recorded with a Hewlett-Packard 8452A Diode array spectrophotometer. Luminescence spectra were recorded with an Aminco-Bowman spectrophotofluorimeter. Irradiation studies were performed using a UV-light source (Hg lamp), and a tungsten (W) lamp, with appropriate band-pass optical filters.

Zinc tetraphenylporphyrin (ZnTPP) was synthesized from purified H_2TTP (chlorin free) [20] and zinc acetate using standard literature techniques [21]. All other chemicals used were of the highest purity available commercially.

3. Results

3.1. Effects of CdS nanoparticles on the absorption spectrum of ZnTPP

The absorption spectra of freshly prepared mixtures of ZnTPP and CdS nanoparticles (3:6:3) in 2-propanol, kept in the dark, exhibit a considerable reduction in the absorbance

of ZnTPP at both 422 nm (Soret band) and 556 nm (Q-band), compared to the spectra of ZnTPP in 2-propanol at the same concentration. The appropriate absorbances (optical densities) of ZnTPP at 422 nm and 556 nm, in the absence and the presence of 3×10^{-4} M CdS nanoparticles (2:4:2) in 2-propanol vs. $[\text{ZnTPP}]$ are shown in Fig. 1. Values of $(\text{O.D.})_{\text{ZnTPP}} - (\text{O.D.})_{\text{ZnTPP}^{\text{CdS}}}$ at 422 nm or the difference in absorbance, shown in Fig. 1(a), exhibit a Langmuir-type leveling-off at higher $[\text{ZnTPP}]$ values. The reduction in the absorbance of ZnTPP in the presence of CdS nanoparticles may be due to the adsorption of ZnTPP molecules onto the surface of the nanoparticles leading to a reduction in the concentration of ZnTPP in the solution. In addition, it may be attributed to a reduction in the value of the molar extinction coefficient of adsorbed ZnTPP molecules, as will be discussed later.

To determine the extent of adsorption of ZnTPP molecules onto the surface of CdS nanoparticles, mixtures of variable concentrations of ZnTPP and a constant concentration of CdS nanoparticles in 2-propanol were subjected to ultrafiltration (100 Å membrane filters) under applied pressure. Absorption spectra of the mixtures were recorded before and after ultrafiltration. In control experiments, the absorption spectrum of ZnTPP in 2-propanol was virtually unaffected by ultrafiltra-

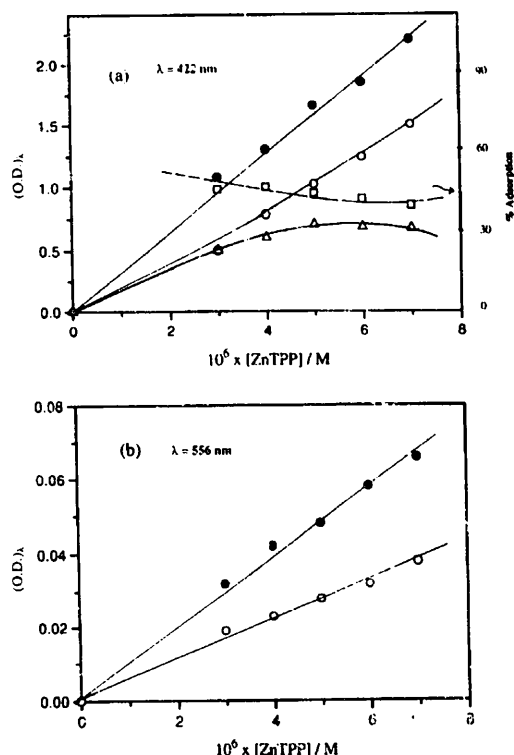


Fig. 1. Absorbance of ZnTPP vs. $[\text{ZnTPP}]$ in 2-propanol at different wavelengths: (●) in the absence of CdS nanoparticles and (○) in the presence of 3×10^{-4} M CdS nanoparticles. (▲) difference in absorbance or optical density of adsorbed ZnTPP; (□) percent adsorption of ZnTPP.

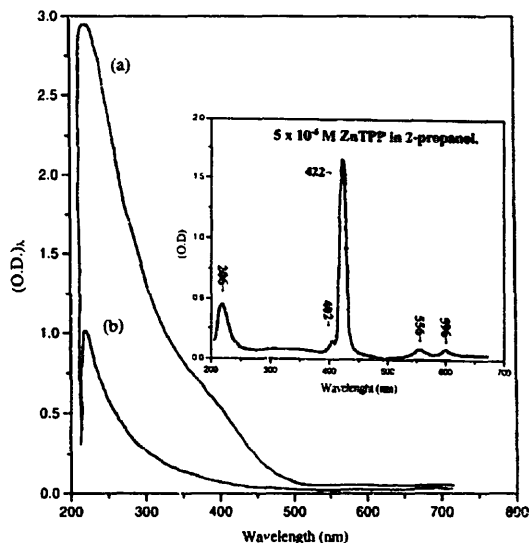


Fig. 2. Absorption spectra of 3×10^{-4} M CdS nanoparticles (2:4:2) in 2-propanol, before (b) and after (a) ultrafiltration (100 Å membrane filters) vs. 2-propanol ($L=1.00$ cm). Inset: absorption spectrum of 5×10^{-6} M ZnTPP in 2-propanol before ultrafiltration (absorption spectrum after ultrafiltration nearly identical).

tion (2–3% retention by the filter). On the other hand, the absorption spectrum of CdS nanoparticles (2:4:2) in 2-propanol was reduced drastically by ultrafiltration. Typical absorption spectra of CdS nanoparticles in 2-propanol before and after ultrafiltration are depicted in Fig. 2. The inset to Fig. 2 shows the absorption spectrum of ZnTPP in 2-propanol before ultrafiltration. The absorption spectrum of ZnTPP recorded after ultrafiltration was nearly identical; it cannot be distinguished from the spectrum before ultrafiltration. The difference in the absorbances of CdS nanoparticles before and after ultrafiltration, namely $(O.D.)_{\lambda}^B - (O.D.)_{\lambda}^A$, is wavelength dependent. The percent retention of CdS nanoparticles by the filter, namely $\{(O.D.)_{\lambda}^B - (O.D.)_{\lambda}^A / (O.D.)_{\lambda}^B\} \times 100$, is plotted vs. the wavelength in Fig. 3. It reaches 95% if determined at 400 nm. Fig. 3 indicates that large CdS nanoparticles ($\lambda_{abs} > 400$ nm) are retained by the filter more effectively than smaller nanoparticles ($\lambda_{abs} < 360$ nm). Although the absorbance of CdS nanoparticles becomes quite small at $\lambda > 460$ nm and the percent retention determined at $\lambda > 460$ nm may involve a significant error, the error is negligible in the range of 360–440 nm.

Variable concentrations of ZnTPP, ranging from 2×10^{-6} M to 1×10^{-5} M, were mixed with 2×10^{-4} M CdS nanoparticles (2:4:2) in 2-propanol and they were kept in the dark for 1 h. Their absorption spectra were recorded before and after ultrafiltration. The absorbance of the mixture at 360 nm, 422 nm and at 556 nm, plotted vs. [ZnTPP], was found to decrease by ultrafiltration (Fig. 4(a)–4(c)). The absorbance at 360 nm is attributed mainly to CdS nanoparticles. The contribution of ZnTPP in the absorbance at 360 nm is small even at the highest [ZnTPP] used and it is manifested in the

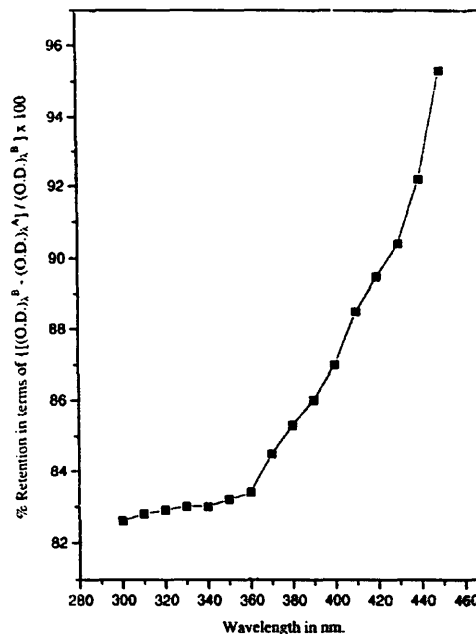


Fig. 3. Plots of % retention of 3×10^{-4} M CdS nanoparticles (2:4:2) by ultrafiltration vs. λ (nm).

slight increase in the value of $(O.D.)_{360}$ of the filtrate at high [ZnTPP]. The absorbance at 422 nm is attributed to ZnTPP with some small contribution from larger CdS nanoparticles (5% at the highest [ZnTPP] used, before ultrafiltration). Finally the absorbance at 556 nm is attributed primarily to ZnTPP. The differences in the absorbance of ZnTPP at 422 nm and at 556 nm before and after ultrafiltration, $(O.D.)_{\lambda}^B - (O.D.)_{\lambda}^A$, level-off at high [ZnTPP]. Limiting values of $\Delta(O.D.)_{\lambda}$ at 1×10^{-5} M ZnTPP, namely 0.37 at 422 nm and 0.009 at 556 nm, imply that approximately 1.3×10^{-6} M ZnTPP is adsorbed on the retained CdS nanoparticles (95%) based on $\Delta(O.D.)_{422}$ and approximately 9.3×10^{-7} M ZnTPP based upon $\Delta(O.D.)_{556}$. The former value of $[ZnTPP]_{ads}$ may not be exact. It requires three minor corrections. The value of $\Delta(O.D.)_{422}$ should be reduced by the absorbance of about 5% CdS nanoparticles in the filtrate at 422 nm, namely by 0.008. In addition, very small CdS nanoparticles may be present in the filtrate and they may carry ZnTPP molecules. Furthermore, the molar extinction coefficient of ZnTPP at 422 nm used to calculate $[ZnTPP]_{ads}$ from the value of $(O.D.)_{422}^B - (O.D.)_{422}^A$ was that of ZnTPP in the absence of CdS nanoparticles, which is slightly higher than the molar extinction coefficient of ZnTPP adsorbed onto CdS (see Section 4). On the other hand, the value of $\Delta(O.D.)_{556}$ is subject to a more significant error due to the low absolute values of $(O.D.)_{556}$ before and after ultrafiltration. Therefore, an approximate value of $[ZnTPP]_{ads}$ equal to 1.3×10^{-6} M ZnTPP is considered as an upper limit under the conditions described above, leading to $[ZnTPP]_{ads} / [CdS] \sim 6.5 \times 10^{-3}$ and to $[ZnTPP]_{ads} / [ZnTPP]_0 \sim 0.13$.

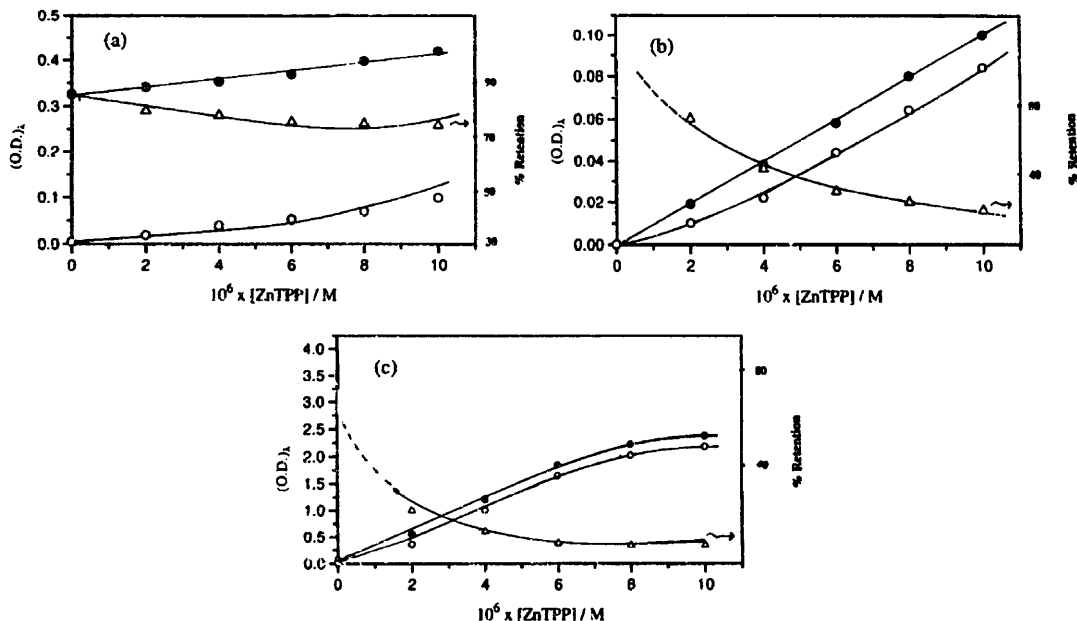


Fig. 4. Variation of the absorbance of ZnTPP in the presence of $2 \times 10^{-4} \text{ M}$ CdS nanoparticles in 2-propanol at different wavelengths vs. $[\text{ZnTPP}]$ (●) Before ultrafiltration; (○) After ultrafiltration; (Δ) $\{[(\text{O.D.})_{\lambda}^{\text{h}} - (\text{O.D.})_{\lambda}^{\text{b}}] \times 100 / (\text{O.D.})_{\lambda}^{\text{h}}\}$ or % retention by membrane filters. (a) $\lambda = 360 \text{ nm}$; (b) $\lambda = 556 \text{ nm}$; (c) $\lambda = 422 \text{ nm}$.

i.e. approximately 13% adsorption. If the average-size CdS nanoparticle consists of m CdS units then approximately $6.5 \times 10^{-3} \times m$ ZnTPP molecules are adsorbed per average-size nanoparticle. Values of m equal to 200 CdS units imply that at least one ZnTPP molecule is adsorbed per CdS particle.

3.2. Irradiation of ZnTPP with visible light in the presence of CdS nanoparticles

Although solutions of ZnTPP in 2-propanol are completely stable photochemically, even under drastic UV and visible light irradiation in the presence of O_2 , the presence of CdS nanoparticles renders ZnTPP very active photochemically. Mixtures of ZnTPP and CdS nanoparticles in 2-propanol had to be kept in the dark, at near zero temperature ($^{\circ}\text{C}$), before scheduled experiments could be carried out. Room light induces drastic changes in the absorption spectrum of ZnTPP in the presence of CdS nanoparticles. Some of the changes brought about by room light are depicted in Fig. 5. A strong and broad absorption band in the range of 700–900 nm is attributed to intermediate photoproducts whose lifetime is a few hours. Absorption bands in the range of 600–700 nm are attributed to somewhat more stable photoproducts whereas absorption bands at about 520 nm and 580 nm represent fairly stable photoproducts. At the same time the Soret band (422 nm) and the Q-band (556 nm) of ZnTPP disappear almost completely, indicating complete photodecomposition of ZnTPP. However, irradiation by room light leads to a very complicated photochemistry of ZnTPP in the presence of CdS

nanoparticles. Room light brings about electronic excitation of both CdS and ZnTPP. Excited CdS, namely $\text{CdS}(e^-/h^+)$, lead to the formation of both ZnTPP^- and O_2^- , in addition to $(\text{CH}_3)_2\dot{\text{C}}\text{-OH}$ (hole transfer). On the other hand, $^1\text{ZnTPP}^*$ may lead to ZnTPP^+ and $\text{CdS}(e^-)$, in the presence of fairly large CdS nanoparticles [9,12], if back electron transfer from adsorbed ZnTPP^+ to $\text{CdS}(e^-)$ does not dominate. It is apparent that the resulting photochemistry is too complicated to be elucidated successfully.

3.3. Ultraviolet irradiation of ZnTPP in the presence of CdS nanoparticles

Ultraviolet irradiation of mixtures of ZnTPP and CdS nanoparticles in 2-propanol, using a Hg lamp, leads primarily to the electronic excitation of CdS nanoparticles at 360 nm, although a very small portion of ZnTPP molecules also gets excited to $^1\text{ZnTPP}^*$ at the highest $[\text{ZnTPP}]$ used, namely $2 \times 10^{-5} \text{ M}$ at this wavelength. In addition, ZnTPP molecules are excited at $410 \pm 10 \text{ nm}$ and by the visible components of the Hg lamp. Absorption spectra of $2 \times 10^{-5} \text{ M}$ ZnTPP in the presence of $3 \times 10^{-4} \text{ M}$ CdS nanoparticles in 2-propanol, irradiated by the UV lamp for various time intervals, are shown in Fig. 6. The absorbance of ZnTPP at 422 nm and 556 nm decreases drastically with irradiation time. Both absorption bands disappear completely after 100 min of irradiation. A broad absorption band at 700–850 nm builds up with irradiation time, reaches a maximum at about 15 min and then it decreases until it disappears completely (120

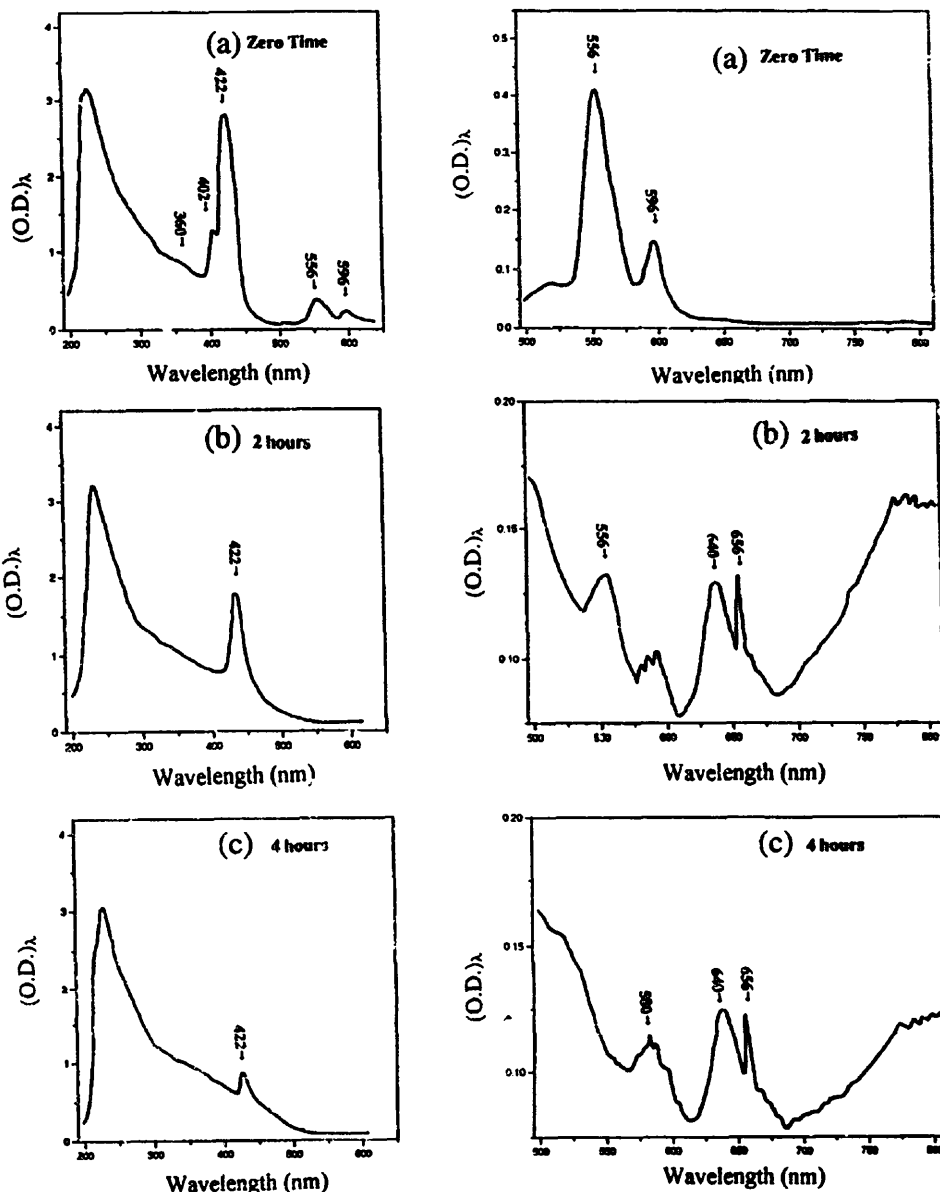


Fig. 5. Absorption spectra of 2×10^{-5} M ZnTPP and 3×10^{-4} M CdS nanoparticles (2:4:2) in 2-propanol (air-saturated) exposed to room light for variable time intervals. (a) Zero time (b) 2 h exposure (c) 4 h exposure ($L = 1.00$ cm).

min). A similar pattern is observed with the absorption band at 636 nm which is replaced by a broader band at about 640 nm. Finally, absorption bands which appear to be linked to stable photoproducts are building-up with irradiation time in the spectral ranges of 300–400 nm, 500–520 nm, 580 nm and 640 nm. It is apparent that short irradiation times give rise to the formation of intermediate photoproducts characterized by absorption bands at 636 and 700–850 nm, where as long irradiation times lead to more stable photoproducts. Prolonged UV irradiation leads to the complete disappearance

of all absorption bands at $\lambda > 400$ nm. However, the resulting photochemistry under such irradiation conditions is still very complex because it may involve both CdS (e^-/h^+) interacting with ZnTPP and O_2 as well as $^1\text{ZnTPP}^*$ interacting with CdS nanoparticles. The result of such interactions could be the formation of ZnTPP^- , ZnTPP^+ , $\text{CdS}(e^-)$, $\text{CdS}(h^+)$ and O_2^- . Obviously, one has to selectively excite either CdS only or ZnTPP, to simplify the photochemistry involved.

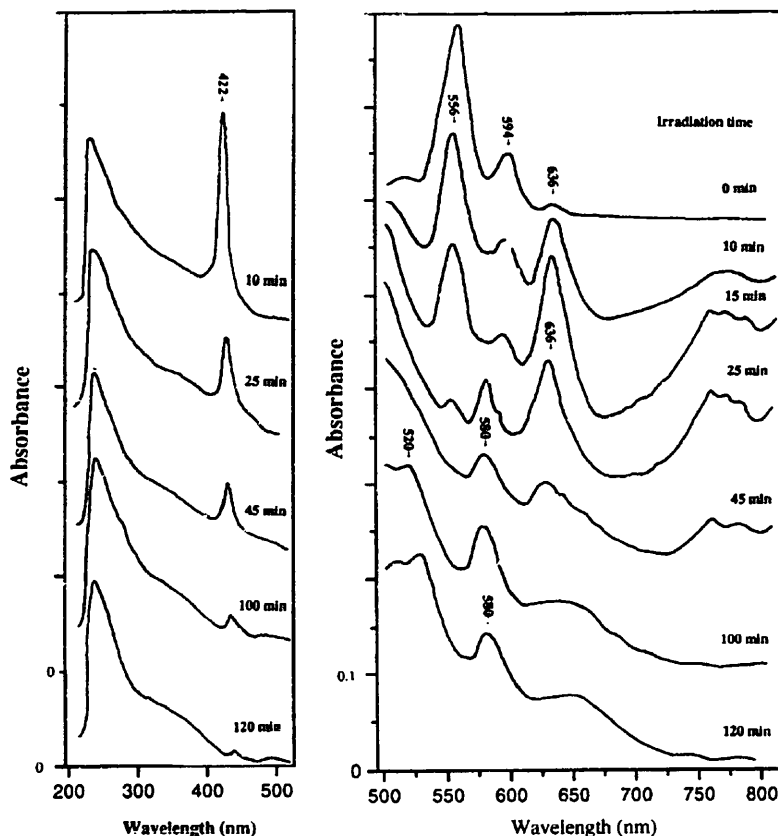
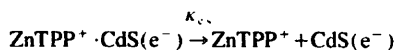
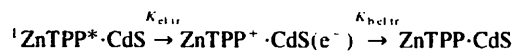


Fig. 6. Absorption spectra of 2×10^{-5} M ZnTPP and 3×10^{-4} M CdS nanoparticles (2:4:2) in 2-propanol, irradiated at 360 ± 10 nm for different time intervals vs. 2-propanol. $E_g = 2.95$ eV; air-saturated solutions ($L = 1.00$ cm).

3.4. Irradiation of ZnTPP in the presence of CdS nanoparticles at $\lambda > 515$ nm

To simplify the photochemistry of ZnTPP in the presence of CdS nanoparticles, mixtures of ZnTPP and CdS nanoparticles in 2-propanol were irradiated with a W lamp through a long pass color glass filter ($\lambda_{\text{trans}} > 515$ nm, Oriel 59502) in the absence of O_2 . Under these conditions only ZnTPP molecules are excited to $^1\text{ZnTPP}^*$, through their Q-bands since CdS nanoparticles are completely transparent at $\lambda > 515$ nm. Electronically excited ZnTPP molecules ($^1\text{ZnTPP}^*$) are partially quenched by CdS nanoparticles characterized by $E_g < 3.0$ eV [11,12]. The fluorescence quenching of ZnTPP by such CdS nanoparticles is attributed to electron transfer from $^1\text{ZnTPP}^*$ molecules adsorbed onto the surface of CdS nanoparticles to the conduction band of the nanoparticle.



where $k_{\text{el.tr}}$, $k_{\text{h.el.tr}}$ and $k_{\text{c.}}$ are appropriate rate constants for electron transfer, back electron transfer and charge separa-

tion, respectively. The formation of ZnTPP^+ and $\text{CdS}(e^-)$ leads to additional thermal reactions.

Absorption spectra of deaerated mixtures of 2×10^{-5} M ZnTPP and 3×10^{-4} M CdS ($E_g \approx 2.9\text{--}3.1$ eV) in 2-propanol, irradiated at $\lambda > 515$ nm for various time intervals, exhibit a very minor initial decrease in the absorbance of the Soret band (422 nm) and the Q-bands (556 and 596 nm), accompanied by a slight increase in the absorbance of the irradiated sample in the spectral ranges 325–360 nm, 450–500 nm and 402 nm. These minor changes are consistent with the formation of traces of zinc tetraphenylporphyrin radical cation, $\text{ZnTPP}^+ \cdot \text{ClO}_4^-$ [22,23], accompanied by a parallel destruction of ZnTPP (3–4%), monitored by the absorbance at 536 nm. The emission spectra of ZnTPP in the irradiated samples, excited at either 360 nm or 544 nm, remain virtually unchanged. The fluorescence intensity ratio $(I_F)_{600}/(I_F)_{650}$ is unaffected by irradiation under moderate conditions (up to 80 min). However, prolonged irradiation at $\lambda > 515$ nm (120–150 min) leads to an increase in the absorbances at 422 nm, 556 nm and 596 nm to values slightly higher than those of the unirradiated samples. In addition, both the intensity of the recombination luminescence of CdS nanoparticles and

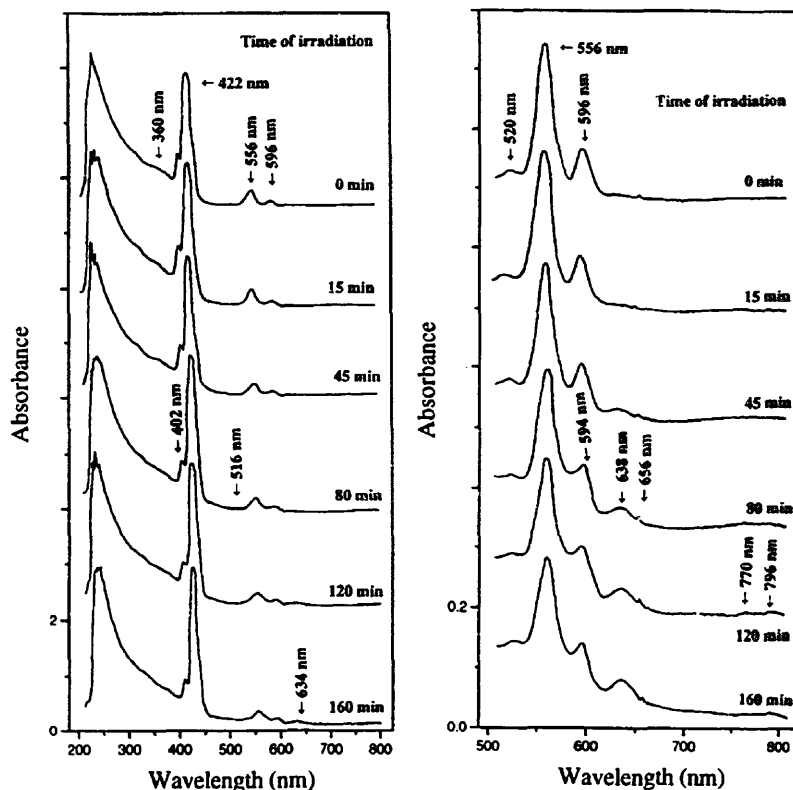


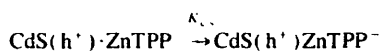
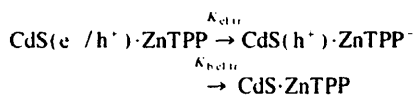
Fig. 7. Absorption spectra of 2×10^{-4} M ZnTPP in the presence of 3×10^{-4} M CdS nanoparticles (2:4:2) in 2-propanol, irradiated at 434 ± 10 nm for different time intervals vs. 2-propanol; deaerated solutions ($L = 1.00$ cm).

the fluorescence intensity ratio, $(I_F)_{600}/(I_F)_{650}$, decrease at long irradiation times. The presence of O_2 during irradiation does not affect these observations. Therefore, one can safely assume that irradiation of ZnTPP in the presence of CdS nanoparticles characterized by $E_g \approx 2.9$ – 3.1 eV at wavelengths at which CdS is transparent, leads to very negligible photochemistry of ZnTPP under moderate irradiation conditions. Obviously, drastic irradiation conditions and use of CdS nanoparticles characterized by $E_g \sim 2.5$ – 2.8 eV may lead to more extensive photochemistry. However, CdS nanoparticles characterized by $E_g \sim 2.5$ – 2.8 eV are very unstable and precipitate out. Therefore, photooxidation of $^1\text{ZnTPP}^*$ by CdS nanoparticles used in this work is negligible both in the absence and presence of O_2 .

3.5. Irradiation of ZnTPP in the presence of CdS nanoparticles with near-ultraviolet radiation

Irradiation of mixtures of ZnTPP and CdS nanoparticles in 2-propanol, in the absence of O_2 at 434 ± 10 nm, was employed to lead to the excitation of larger CdS nanoparticles ($E_g \approx 2.9$ – 3.0 eV), although it also led to the excitation of a small fraction of ZnTPP. However, since the nanoparticles used are characterized by $E_g \approx 2.9$ – 3.0 eV, the conclusions

reached earlier regarding the insignificant photochemistry of ZnTPP in the presence of CdS nanoparticles at $\lambda_{\text{irrad}} > 515$ nm are still in effect. Excitation of CdS nanoparticles to CdS (e^-/h^+) at 434 ± 10 nm leads to a photochemical activity of ZnTPP molecules adsorbed onto CdS (e^-/h^+):



Both $\text{CdS}(h^+)$ and ZnTPP^- undergo further reactions as will be discussed later.

The absorption spectra of mixtures of ZnTPP and CdS nanoparticles in 2-propanol, irradiated at 434 ± 10 nm in the absence of O_2 , show a decrease in the absorbance of ZnTPP at 422 nm, 556 nm and 596 nm, nearly to the same extent, accompanied by an increase in the absorbance of the irradiated sample in the spectral ranges of 450–500 nm and 634–638 nm and a gradual formation of a very broad band with a maximum at about 520 nm, under the Q bands of ZnTPP (Fig. 7). The latter absorption bands are consistent with the formation of very small quantities of zinc tetraphenyl porphyrin radical anion, ZnTPP^- , coupled with either Na^+ or

Cd^{2+} in the dispersion system, or the formation of ZnTPPH^+ [24,25] characterized by an absorption maximum at 457 nm. Disproportionation of ZnTPP^- or ZnTPPH^+ leads to the recovery of ZnTPP (50%) and formation of reduced ZnTPP whose nature will be discussed later. The latter compound may be responsible for the broad absorption band under the Q-bands of ZnTPP .

Although the presence of O_2 does not affect the photochemistry of ZnTPP molecules adsorbed onto CdS nanoparticles and irradiated at $\lambda > 515$ nm, it affects the absorption spectra of the mixture of ZnTPP and CdS nanoparticles irradiated at 434 ± 10 nm, drastically. Typical absorption spectra of irradiated samples are depicted in Fig. 8. The absorbance of ZnTPP at 422 nm, 556 nm and 596 nm decreases drastically with irradiation time, whereas that at 360 nm increases very slightly. A broad absorption band in the range of 700–900 nm increases gradually with time, reaches a maximum and then it decreases. Another broad band with a maximum in the range of 634–640 nm (shifting to longer wavelengths at longer times) exhibits a similar behavior. Finally, a broad absorption band is gradually developing at $\lambda < 600$ nm with λ_{max} at about 520 nm. Since the extent of excitation of CdS nanoparticles at 436 ± 10 nm is rather low, it takes long irra-

diation times to photodecompose ZnTPP effectively, namely 90–100 min for 50% conversion. At such long irradiation times thermal effects may become significant, although the outer jacket of the reaction cell was filled with water to avoid such thermal effects. To separate and characterize the photoproducts formed, more effective excitation conditions are required, i.e. 360 ± 10 nm. The irradiation time can be reduced to 10–20 min (see Fig. 6) for quantitative photochemical conversion of ZnTPP in the presence of CdS nanoparticles under such conditions, without risking thermal effects.

The emission spectra of ZnTPP – CdS mixtures irradiated at 434 ± 10 nm exhibit features which are different than those of unirradiated ZnTPP . At $\lambda_{\text{exc}} = 544$ nm, the fluorescence intensity ratio $(I_F)_{600}/(I_F)_{650}$ decreases slowly with irradiation time and the emission band at 650 shifts slowly to shorter wavelengths (645 nm). The change in the emission spectra of the irradiated sample is more pronounced at $\lambda_{\text{exc}} = 360$ nm (Fig. 9). The recombination luminescence of CdS nanoparticles, monitored at 525 nm, where ZnTPP is transparent, decreases with irradiation time. The $(I_F)_{600}/(I_F)_{650}$ ratio decreases even more markedly at $\lambda_{\text{exc}} = 360$ nm. At long irradiation times the emission band at 600 nm is reduced by

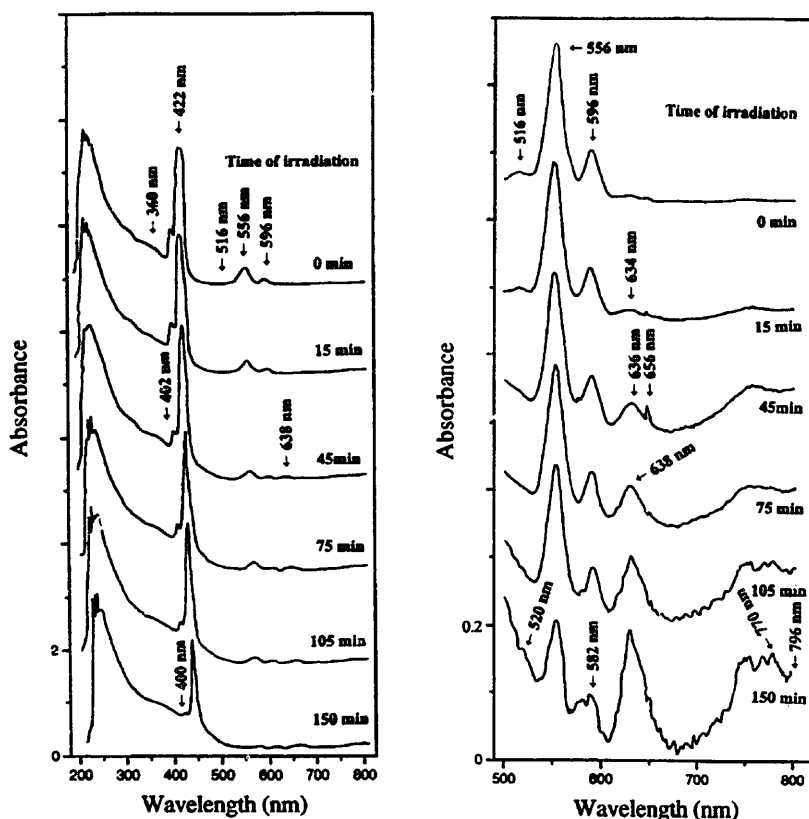


Fig. 8. Absorption spectra of 2×10^{-5} M ZnTPP in the presence of 3×10^{-4} M CdS nanoparticles (3:6:3) in 2-propanol, irradiated at 434 ± 10 nm for different time intervals vs. 2-propanol: air-saturated solutions ($L = 1.00$ cm).

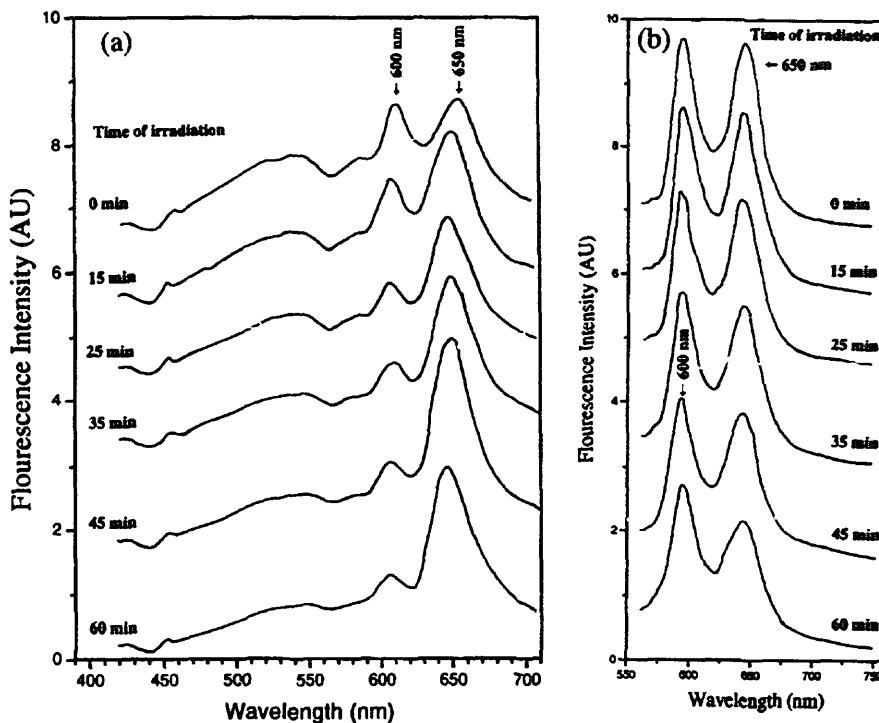


Fig. 9. Emission spectra of 2×10^{-5} M ZnTPP in the presence of 3×10^{-4} M CdS nanoparticles (3:6:3) in 2-propanol, irradiated at 434 ± 10 nm for different time intervals; air-saturated solutions: (a) $\lambda_{exc} = 360 \pm 2$ nm. (b) $\lambda_{exc} = 542 \pm 2$ nm.

more than 50% whereas the band at 650 gains intensity (30–40%), becomes broader and shifts to about 643–644 nm. It is apparent that there are at least two emitting compounds in the irradiated sample, in addition to CdS nanoparticles; ZnTPP and a compound which emits at 643–645 nm and it is excited more effectively at 360 nm than at 544 nm. The intermediate components with absorption bands at 634–640 nm and 700–900 nm either do not fluoresce or their fluorescence is in the far red region of the spectrum and it escaped detection. Furthermore, since irradiation of ZnTPP–CdS at 434 ± 10 nm under these conditions leads to partial photodecomposition of ZnTPP the changes observed in the emission spectra are attributed to intermediate rather than final photoproducts.

4. Discussion

If the absorbance of ZnTPP in the presence of CdS nanoparticles after ultrafiltration represents ZnTPP molecules primarily in solution, namely $[\text{ZnTPP}]_{eq}$ in the mixture of ZnTPP–CdS nanoparticles under equilibrium conditions, and if the difference in the absorbance before and after ultrafiltration, $(\text{O.D.})_{\lambda}^B - (\text{O.D.})_{\lambda}^A$ ($\lambda = 422$ and 556 nm) is converted to $[\text{ZnTPP}]_{init} - [\text{ZnTPP}]_{eq}$ using the molar extinction coefficient of ZnTPP in 2-propanol, then the latter difference represents $[\text{ZnTPP}]_{ads}$, namely the concentration

of ZnTPP adsorbed onto the surface of CdS nanoparticles. In this approach, $[\text{ZnTPP}]_{init}$ represents the initial concentration of ZnTPP which is distributed between ZnTPP in solution and ZnTPP adsorbed onto the surface of CdS nanoparticles. Plots of $[\text{ZnTPP}]_{ads}$ vs. $[\text{ZnTPP}]_{eq}$ should give rise to Langmuir-type curves, whose limiting values should represent the amount of ZnTPP adsorbed onto the surface of the fixed quantity of CdS used. Such plots are illustrated in Fig. 10(a) and 10(b). Limiting values of $[\text{ZnTPP}]_{ads}$ resulting from these curves, namely 9×10^{-7} M ZnTPP ($\lambda = 556$) and 1.3×10^{-6} M ZnTPP ($\lambda = 422$ nm), are in close agreement with values obtained from the plots of $\Delta(\text{O.D.})_{\lambda}$ vs. $[\text{ZnTPP}]$, illustrated in Fig. 4(b) and 4(c). However, the former value (9×10^{-7} M) is considered to involve more significant errors, as was discussed earlier.

It was mentioned earlier that the results depicted in Fig. 1 can be accounted for in terms of a reduction in the value of the molar extinction coefficient(s) of ZnTPP adsorbed onto the surface of CdS nanoparticles. From the absorption spectra before and after ultrafiltration one can record the following:

$$[\text{ZnTPP}]_{ads} = [\text{ZnTPP}]_{initial} - [\text{ZnTPP}]_{eq}$$

and

$$(\text{O.D.})_{\lambda}^{ads} = (\text{O.D.})_{\lambda}^B - (\text{O.D.})_{\lambda}^A = \Delta(\text{O.D.})_{\lambda}$$

Plots of $(\text{O.D.})_{\lambda}^{ads}$ ($\lambda = 422$ and 556 nm) vs. $[\text{ZnTPP}]_{ads}$ lead to the values of the apparent molar absorptivity of

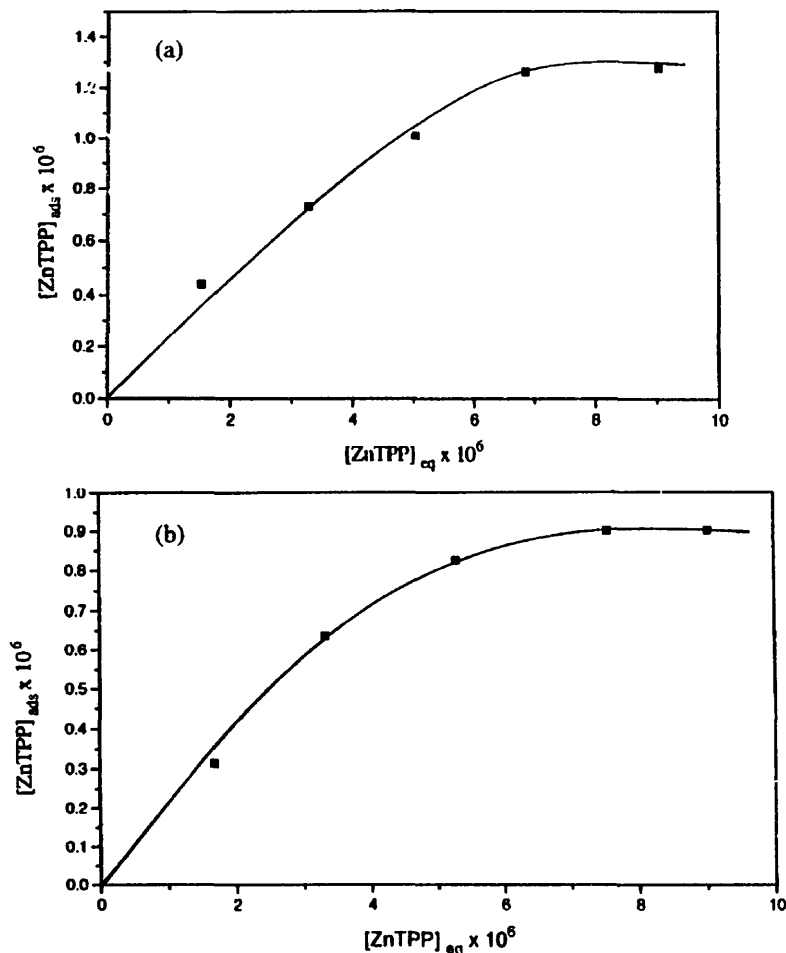
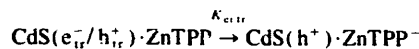


Fig. 10. Plots of $[\text{ZnTPP}]_{\text{ads}}$ vs. $[\text{ZnTPP}]_{\text{eq}}$ of ZnTPP in the presence of 2×10^{-4} M CdS nanoparticles (2:4:2) in 2-propanol. (a) Calculated from $(\text{O.D})_{422}^{\text{B}} - (\text{O.D})_{422}^{\text{A}}$; (b) calculated from $(\text{O.D})_{434}^{\text{B}} - (\text{O.D})_{434}^{\text{A}}$. Values of $[\text{ZnTPP}]_{\text{eq}}$ were calculated from the corresponding values of $(\text{O.D})_{\lambda}^{\text{A}}$ and ϵ_{λ} (ZnTPP).

adsorbed ZnTPP molecules onto the surface of CdS nanoparticles (Fig. 1). From the slope of Fig. 1 we obtain $\epsilon_{\text{app}}(422) = 2.11 \times 10^5 \text{ M}^{-1} \text{ cm}^{-1}$, which compares with $\epsilon_{422}(\text{ZnTPP}) = 3.2 \times 10^5 \text{ M}^{-1} \text{ cm}^{-1}$ for free ZnTPP in 2-propanol. Therefore, there is a reduction in the molar absorptivity of ZnTPP at 422 nm upon adsorption onto CdS nanoparticles equal to approximately 34%.

Electronic excitation of CdS nanoparticles at 434 ± 10 nm, in the presence of ZnTPP, leads to electron transfer from the conduction band of CdS to adsorbed ZnTPP molecules.



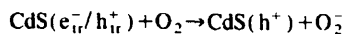
$$\Delta G_{\text{cl,ir}}^{\circ} = eE^{\circ}(\text{CdS}(h^+)/\text{CdS}(e_{\text{ir}}^-/h_{\text{ir}}^+)) - eE^{\circ}(\text{ZnTPP}/\text{ZnTPP}^-) - e^2/\epsilon R \approx 0 \text{ eV}$$

based on $E^{\circ}(\text{ZnTPP}/\text{ZnTPP}^-) = -1.07 \text{ V}$ vs. NHE [24] and $E^{\circ}(\text{CdS}(h^+)/\text{CdS}(e_{\text{ir}}^-/h_{\text{ir}}^+)) = -1.07 \text{ V}$ vs. NHE in 2-

propanol (for CdS nanoparticles with diameters about 45 Å). The electron transfer event is accompanied by either back electron transfer from ZnTPP^- to $\text{CdS}(h^+)$, which is very efficient,

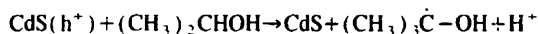
$$\Delta G_{\text{b,el,ir}}^{\circ} = eE^{\circ}(\text{ZnTPP}/\text{ZnTPP}^-) - eE^{\circ}(\text{CdS}(h^+)/\text{CdS}) = -3.1 \text{ eV} \quad (5)$$

based on $E^{\circ}(\text{CdS}(h^+)/\text{CdS}) \sim 1.90 \text{ V}$ vs. NHE [1] (for CdS nanoparticles with 45 Å diameters), or by charge separation leading to $\text{CdS}(h^+)$ plus ZnTPP^- . In the presence of O_2 (air-saturated solutions), molecular oxygen competes against ZnTPP for e_{CB}^- from CdS ($e_{\text{ir}}^-/h_{\text{ir}}^+$)



$$\Delta G_{\text{cl,ir}}^{\circ} = eE^{\circ}(\text{CdS}(h^+)/\text{CdS}(e_{\text{ir}}^-/h_{\text{ir}}^+)) - eE^{\circ}(\text{O}_2/\text{O}_2^-) = -0.5 \text{ eV}$$

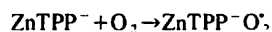
(for CdS nanoparticles with 45 Å diameters). The photo-oxidized CdS(h^+) undergoes hole transfer to 2-propanol:



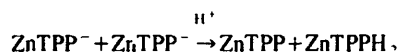
$$\Delta G_{\text{cl.tr}}^0 = eE^0((\text{CH}_3)_2\dot{\text{C}}-\text{OH} / (\text{CH}_3)_2\text{CHOH}) - eE^0(\text{CdS}(h^+) / \text{CdS}) \leq 0 \text{ eV}$$

Although electron transfer from CdS(e^-/h^+) to ZnTPP involves ZnTPP molecules adsorbed onto the surface of CdS nanoparticles, whose concentration is at most 1.3×10^{-6} M under the conditions of this study, the actual photochemistry of ZnTPP takes place most likely in the solution as it is manifested from the irradiation of deaerated mixtures.

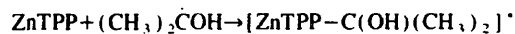
The photochemistry of ZnTPP irradiated at 434 ± 10 nm in the presence of CdS nanoparticles involves the formation of at least three radical ions or free radicals: ZnTPP^- ($\lambda_{\text{abs}} = 455\text{--}457$ nm [25,26]), O_2^- and $(\text{CH}_3)_2\dot{\text{C}}\text{OH}$. The metalloporphyrin radical anion participates in additional reactions such as:



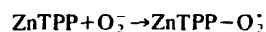
leading to the formation of a complex free radical whose absorption spectrum may be in the range of 650–900 nm, disproportionation leading to the reduction of ZnTPP



and

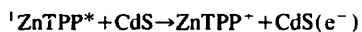


The latter complex may be stable long enough to lead to the absorption spectra observed in the red region of the spectrum. In addition, O_2^- may react with ZnTPP



Obviously, complexes like $\text{ZnTPP}-\text{O}_2^*$ and $[\text{ZnTPP}-\text{C}(\text{OH})(\text{CH}_3)_2]^*$ may be involved in further reactions which may lead to ring opening, demetallation and formation of substituted ZnTPP and reduction of ZnTPP. Photo-oxygenation of metalloporphyrins observed with porphyrins whose $E_{\text{ox}} < 0.4\text{--}0.5$ V led to products with λ_{abs} at 450 nm, 770 nm and 850 nm (open macrocyclic structures) [27,28]. Isolation and chemical identification of both intermediate and final photoproducts, formed under efficient irradiation conditions, is needed to elucidate the photochemistry of ZnTPP in the presence of CdS nanoparticles.

Excitation of ZnTPP at either 434 ± 10 nm or at $\lambda > 515$ nm, in the presence of CdS nanoparticles ($E_g \approx 2.9$ to 3.1 eV), either does not lead to electron transfer from $^1\text{ZnTPP}^*$ to the conduction band of CdS nanoparticles:



$$\Delta G_{\text{cl.tr}}^0 = eE^0(\text{ZnTPP}^+ / ^1\text{ZnTPP}^*) - eE^0(\text{CdS}/\text{CdS}^-) > 0 \text{ eV}$$

or it involves efficient back electron transfer which negates the effect of electron transfer event, as discussed earlier. The excited triplet state of ZnTPP ($^3\text{ZnTPP}^*$) is rather unlikely to participate in electron transfer to CdS nanoparticles, since

$$E^0(\text{ZnTPP}^+ / ^3\text{ZnTPP}^*) > E^0(\text{ZnTPP}^+ / ^1\text{ZnTPP}^*) > E^0(\text{CdS}/\text{CdS}^-)$$

Detailed NMR, mass spectrometric and GCMS measurements, following irradiation of ZnTPP–CdS mixtures under more drastic and selective conditions, namely at 360 ± 10 nm, and separation of the components through a silica gel column are under way to identify intermediate and final photoproducts, and to elucidate the photochemical mechanism involved [29], which is induced by CdS nanoparticles. The photochemistry of ZnTPP in the presence of CdS nanoparticles appears to be linked to direct or indirect reactions with conduction band electrons (e_{CB}^-) rather than electron transfer from $^1\text{ZnTPP}^*$ to CdS. The role of hole transfer from CdS(h^+) to $(\text{CH}_3)_2\text{CHOH}$ and subsequent reactions of $(\text{CH}_3)_2\dot{\text{C}}\text{OH}$ with ZnTPP needs to be elucidated.

References

- [1] L.E. Brus, *J. Phys. Chem.* 79 (1983) 5560; 80 (1984) 4403.
- [2] A. Henglein, *Pure Appl. Chem.* 56 (1984) 1215.
- [3] M. Grätzel, *Heterogeneous Photochemical Electron Transfer*, CRC Press, Boca Raton, FL, 1989.
- [4] P.V. Kamat, *Chem. Rev.* 93 (1993) 267.
- [5] M.A. Fox, M.T. Dulay, *Chem. Rev.* 93 (1993) 341.
- [6] H. Weller, A. Eychmüller, *Advances in Photochem.* 20 (1995) 165.
- [7] A.P. Alivisatos, *J. Phys. Chem.* 100 (1996) 13226.
- [8] Y.F. Lee, M. Olshavsky, *J. Chrysochoos, J. Less. Comm. Metals* 148 (1989) 259.
- [9] J. Chrysochoos, *J. Molec. Cryst. Lig. Crystals* 194 (1990) 247.
- [10] J. Chrysochoos, *J. Lumin.* 48/49 (1991) 709.
- [11] J. Chrysochoos, *J. Phys. Chem.* 96 (1992) 2868.
- [12] Bhamro, J. Chrysochoos, *J. Lumin.* 60/61 (1994) 359.
- [13] A.V. Isarov, *J. Chrysochoos, Langmuir* 13 (1997) 3142.
- [14] P.V. Kamat, S. Das, K.G. Thomas, M.G. George, *Chem. Phys. Lett.* 178 (1991) 75.
- [15] P.V. Kamat, J.P. Chauvet, R.W. Fessenden, *J. Phys. Chem.* 90 (1986) 1389.
- [16] M.L. Steigerwald, L.E. Brus, *Acc. Chem. Res.* 23 (1990) 183.
- [17] R. Rossetti, K. Hall, J.M. Gibson, L.E. Brus, *J. Chem. Phys.* 82 (1985) 552.
- [18] J.J. Pankove in *Optical Properties of Semiconductors*, Prentice-Hall, Englewood Cliffs, NJ, 1971.
- [19] Y. Wang, A. Suna, W. Mahler, R.I. Kasowski, *J. Chem. Phys.* 87 (1987) 7315.
- [20] G.H. Barnett, M.F. Hudson, K.M. Smith, *Tetrahedron Lett.* (1973) 2887.
- [21] A.D. Adler, F.R. Longo, F. Kampas, J. Kim, *J. Inorg. Nucl. Chem.* 32 (1970) 2443.
- [22] J. Fajer, D.C. Borg, A. Forman, D. Dolphin, R.H. Felton, *J. Am. Chem. Soc.* 92 (1970) 3451.
- [23] W. Potter, R.N. Young, G. Levin, *J. Am. Chem. Soc.* 102 (1980) 2471.

- [24] R.H. Felton, H. Linschitz, *J. Am. Chem. Soc.* 113 (1966) 88.
- [25] G.L. Closs, L.E. Closs, *J. Am. Chem. Soc.* 85 (1963) 818.
- [26] V.S. Chirvony, G.N. Sonyakov, R. Gadonas, K. Vytautas, A. Pelakauskas, *Photochem. Photobiol.* 52 (1990) 697.
- [27] J.-H. Fuhrhop, D. Mauzerall, *Photochem. Photobiol.* 13 (1971) 453.
- [28] P.K.W. Wasser, J.-H. Fuhrhop, *Ann. New York Acad. Sci.* 206 (1973) 533.
- [29] Bhamro, J. Chrysochoos, to be published.